JOURNAL OF MATERIALS SCIENCE 22 (1987) 87–94

On the mixtures $FeCo_MAs_{M'}$ and $CoNi_MAs_{M'}$ and their binding

M. EL-BORAGY, M. ELLNER, K. SCHUBERT
Max-Planck-Institut für Metallforschung, Institut für Werkstoffwissenschaften, Seestrasse 75, 7000 Stuttgart, FRG

Isothermal sections of the phase diagrams $FeCo_MAs_{M'}$ and $CoNi_MAs_{M'}$ have been redetermined. Because of the easy substitution Fe–Co and Co–Ni the marginal phases extend considerably into the three-component range and concomitantly change the axial ratio of their cells. The phase $Fe_{1-N}Co_NAs$, in particular, changes its axial ratio from the long subtype of the MnP type in FeAs continuously to the short subtype in CoAs. An interpretation of the experimental results becomes possible when it is assumed that following Ekman's rule the A atoms iron, cobalt, nickel do not essentially contribute to the valence electron correlation with cell *b*, and that the d electrons of the A atoms form a correlation of their own with cell *e*, not comprising the d electrons of arsenic. A phase becomes stable when there is favourable commensurability between the cells *b*, *e*, *c* of the different spatial correlations of the electrons and the cell *a* of the structure. From the binding interpretation emerge new arguments for the long and the short subtype of the MnP type, for the magnetic saturation moments of the elements iron, cobalt, nickel, and for other phenomena.

1. Introduction

The phase diagrams $FeAs_M$ (M = undetermined mole number) [1], $CoAs_M$ [2], $NiAs_M$ [3] were early determined and crystal structures of their phases such as NiAs(H2.2) [4], $CoAs_3$(B4.12) [5], or $Fe_2As(Cu_2Sb)$ [6, 7] were soon afterwards analysed (for structure type symbols see [8, 9]). However, attempts to find a chemical (i.e. energetical) understanding of the phase diagrams and intermediate phases have not been very successful so far. A method helpful for finding an energetical interpretation of an alloy is to consider the results of small variations of the bonding, realized by alloying quasi homologic mixtures such as $FeAs_M$ and $CoAs_M$ or $CoAs_M$ and $NiAs_M$. The change of the elementary cell with the composition of a phase and also the extension of the range of homogeneity may give indications in favour of an assumed bonding type (binding).

The phase diagram, $FeCo_MAs_{M'}$ [10] contains extended ranges of homogeneity of the marginal phases caused by the easy substitution Fe–Co. The determination of cells of some three-component compositions of these phases was desirable and also the confirmation of a three-component phase proposed by Naud and Breckpot [10].

In the phase diagram $CoNi_MAs_{M'}$ [10] some cells must also be measured, and additional problems considered. The phase Co_5As_2.h (high temperature phase of the compound Co_5As_2) decomposing eutectoidally below 1140 K [10, 11] is of the Pd_5Sb_2(H30.12, SR35.14 [12]) type [11], therefore the isotypic Ni_5As_2(Pd_5Sb_2, SR35.14, [12]) melting at 1266 K [13] might form, at elevated temperatures, a homogeneous mixture with Co_5As_2.h (SR = structure reports, volume, page). The phase Co_2As.h(Fe_2P; H6.3, SR21.38 [14]) permits an easy substitution Co–Ni, so that a comparison with other phases isotypic to Fe_2P (H6.3, SR23.68 [15]) may be made and the change of axial ratio $|a_3|/|a_1|$ with mole fraction of nickel might be interpreted. The phase Co_2As.r [14, 16] is said to show an orthorhombic superstructure and a substructure axial ratio different from that of Co_2As.h. The phase NiAs(H2.2, SR1.84) permits (see Fig. 5) much nickel to be substituted by cobalt, thereby changing its axial ratio [10, 14]; this fact might be interpreted.

The various phenomena occurring in the above mixtures need an energetical interpretation. The first requirement for this is an interpretation of the marginal phases by assigning to them bindings. Many crystal chemical rules valid for AB_M mixtures have been formulated by the plural-correlations model (see e.g. [17], for A, B see [18]). Therefore the binding analysis may be made with the help of this model. A retranslation of the present interpretation into earlier interpretations may be done by identifying the present correlations with the bands of the earlier models; it is clear that the requirements of the models cause differences between occupations assumed in analyses of the band structure and in binding analyses. The bands have not been successful in the interpretation of the crystal chemistry of alloys as the indispensable computational step of configurational interaction has nearly always been omitted. The plural-correlations model yields hypotheses on how the spatial correlations potentially revealed by such calculations might look like. The more facts are interpreted by such hypotheses the more confirmed the latter become. Nearly all chemical phenomena have been found first

0022–2461/87 $03.00 + .12

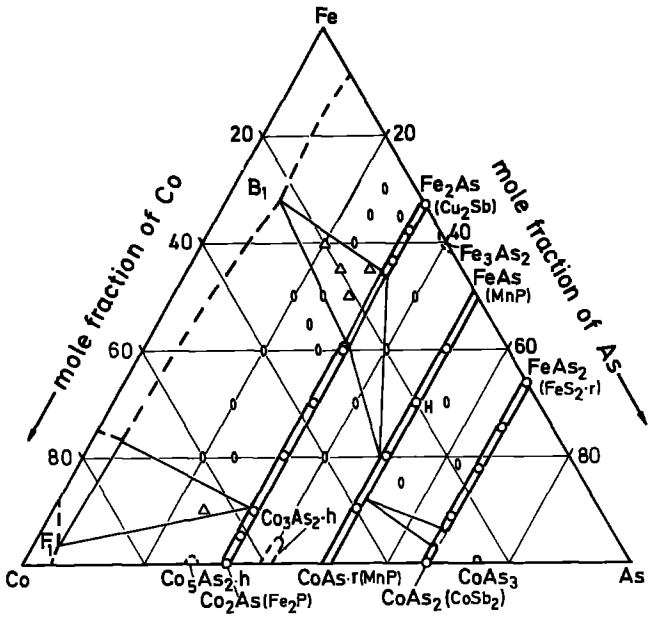

Figure 1 Phase diagram of $FeCo_MAs_{M'}$; 870 K. The alloy $Fe_{30}Co_{20}As_{50}$ has the pseudohexagonal cell H. (○) One-phase, (0) two-phase; (△) three-phase alloy.

by the inductive method and afterwards confirmed by deductive calculations; therefore, it is admissible to discuss hypotheses on bonding types as applied to empirical phenomena. The plural-correlations model is a result of the study of relations between electron numbers and geometry of a structure, a study that unfortunately was neglected in metallurgy after the promising beginnings of Hume-Rothery.

2. Results

The alloys were prepared from iron (99.99%, Ventron), cobalt (99.99%, Ventron), nickel (99.99%, Koch Light), arsenic (99.999%, Koch Light) in evacuated quartz capsules, filled with argon (> 99.99%), by a heat treatment 6 h 550 K, heating up to 1600 K, 0.2 h 1600 K, 12 h 970 K. The powders were annealed (in quartz capillaries filled with argon) 12 h 970 K or 12 h 870 K, and then quenched in water. The powders were examined by the Guinier method with $CoK\alpha_1$ radiation. The constants from measurements of diagrams calibrated with silicon powder were least squares refined using most lines of the photographs.

The isothermal section at 870 K of the phase diagram $FeCo_MAs_{M'}$ drawn following our results in Fig. 1 confirms several results of Naud and Beckpot [10]. The phase $Fe_{2-N}Co_NAs$(Cu_2Sb type) is not very extended, though a weak composition dependence of the axial ratio (Table I, Fig. 2) is exhibited. The cell of $Fe_{2-N}Co_NAs$(Fe_2P type) (Table II, Fig. 3) changes with composition. The phase Co_2As.r (room temperature phase of the compound Co_2As) was confirmed and in Co_2As(14 d 570 K) the existence of superstructure lines seen by Nylund *et al.* [16] was corroborated. The transformation temperature T(h → r) was assumed to be 620 K by Friedrich [3] and 750 K by Heyding [14].

The Fe_3As_2 phase [1] was confirmed by the alloy $Fe_{60}As_{40}$ which did not become liquid after annealing for 4 h at 1150 K, nor was the powder sintered after this treatment. The eutectoidal decomposition of Fe_3As_2 must be quite fast, so that our quenching of the phase was not successful, see phase-diagram Hansen [19] p. 163.

In the section $Fe_{1-N}Co_NAs$ after heat treatment 4 h 1120 K, 12 h 870 K no two-phase range was found near CoAs, as suggested by Naud and Breckpot [10], rather the line diagram of the "long" FeAs(MnP) (see [8] p. 332) transforms continuously to the line diagram of the "short" CoAs.r(MnP) as already found for $Cr_NCo_{1-N}P$, $Mn_NCo_{1-N}P$, $Fe_NCo_{1-N}P$ by Rundqvist [20]; the orthorhombic diagram with a hexagonal axial ratio is found near $Fe_{30}Co_{20}As_{50}$ (see Table III, Fig. 4) while Rundqvist found $Fe_{20}Co_{30}P_{50}$ to be pseudo hexagonal. The non-linear dependence of the cell on mole fraction N'_{Co} near CoAs.r appears remarkable.

The $Fe_{17.5}Co_{20}As_{62.5}$ phase [10] could not be confirmed in the 870 K section.

The $Fe_{1-N}Co_NAs_2$ section is not fully homogeneous as assumed by Naud and Breckpot [10], rather it must

TABLE I Cell of $Fe_{2-N}Co_NAs$(Cu_2Sb type). The number in brackets is the uncertainty of the last figure

Alloy	$\|a_1\|$ (nm)	$\|a_3\|$ (nm)	$\|a_3\|/\|a_1\|$	Reference
$Fe_{66.7}As_{33.3}$	0.3634	0.5985	1.646	SR3.34
$Fe_{60.0}Co_{6.7}As_{33.3}$	0.3633(1)	0.5951(1)	1.638	Present work
$Fe_{55.7}Co_{11.0}As_{33.3}$	0.3634(1)	0.5937(1)	1.634	Present work
$Fe_{50.0}Co_{16.7}As_{33.3}$	0.3631(1)	0.5926(1)	1.632	Present work

TABLE II Cell of Fe_2P type phases. All alloys tempered 12 h 970 K

Alloy	$\|a_1\|$ (nm)	$\|a_3\|$ (nm)	$\|a_3\|/\|a_1\|$
$Co_{66.7}As_{33.3}$	0.5996(1)	0.3578(2)	0.597
$Fe_{5.0}Co_{61.7}As_{33.3}$	0.6031(1)	0.3538(1)	0.587
$Fe_{10.0}Co_{56.7}As_{33.3}$	0.6037(1)	0.3547(1)	0.588
$Fe_{20.0}Co_{46.7}As_{33.3}$	0.6043(1)	0.3558(1)	0.589
$Fe_{30.0}Co_{36.7}As_{33.3}$	0.6057(1)	0.3568(1)	0.589
$Fe_{40.0}Co_{46.7}As_{33.3}$	0.6082(1)	0.3563(1)	0.586
$Co_{60.0}Ni_{6.7}As_{33.3}$	0.5994(1)	0.3564(1)	0.595
$Co_{56.7}Ni_{10.0}As_{33.3}$	0.6042(1)	0.3519(1)	0.582
$Co_{50.0}Ni_{16.7}As_{33.3}$	0.6043(1)	0.3502(1)	0.579
$Co_{40.0}Ni_{26.7}As_{33.3}$	0.6062(1)	0.3483(1)	0.575
$Co_{30.0}Ni_{36.7}As_{33.3}$	0.6076(1)	0.3456(1)	0.569
$Co_{20.0}Ni_{46.7}As_{33.3}$	0.6083(1)	0.3448(1)	0.567

TABLE III Cell of $Fe_{1-N}Co_NAs$ (quenched from 870 K)

Alloy	$\|a_1\|$ (nm)	$\|a_2\|$ (nm)	$\|a_3\|$ (nm)	$\|a_2\|/\|a_1\|$	Reference
$Fe_{50}Co_{00}As_{50}$	0.3373	0.6028	0.5438	1.79	SR3.18
$Fe_{40}Co_{10}As_{50}$	0.3408(1)	0.5981(1)	0.5371(1)	1.75	Present work
$Fe_{30}Co_{20}As_{50}$	0.3436(1)	0.5948(1)	0.5318(1)	1.73	Present work
$Fe_{20}Co_{30}As_{50}$	0.3466(1)	0.5907(1)	0.5280(1)	1.70	Present work
$Fe_{10}Co_{40}As_{50}$	0.3490(1)	0.5889(1)	0.5280(1)	1.69	Present work
$Fe_{00}Co_{50}As_{50}$	0.3492(1)	0.5871(1)	0.5288(1)	1.68	Present work
	0.351	0.596	0.517	1.70	SR3.17 [48]
	0.3458	0.5869	0.5292	1.70	SR21.39 [14]
	0.3489(1)	0.5868(1)	0.5287(1)	1.68	SR37.14 [52]

have a two-phase region separating $CoAs_2$ from the orthorhombic part of the section. In this part a transition from the "long" $FeAs_2$ to the "short" type (see [8] p. 342) is found, the pseudo hexagonal composition being assessed near $Fe_{13}Co_{20}As_{67}$.

The isothermal section of the phase diagram $CoNi_MAs_{M'}$ (Fig. 5) confirms several results found earlier [10]. Fig. 6 suggests that above 1120 K there is homogeneity between Co_5As_2.h and Ni_5As_2. The axial ratio does not appreciably differ from the values given earlier by the cells a = (H0.6825; 1.2513) nm [12] and a = (H0.6797; 1.2423) nm [11]; (H = hexagonal; abbreviated cell notation following Schubert [9, 17]). Alloy $Co_{25}Ni_{46}As_{29}$ (1 d 970 K) contained weak lines of an unknown phase.

The $Co_{67-N}Ni_NAs_{33}$ phase (see Fig. 5) has the cell described in Table II and in Fig. 3. For $N < 0.10$ the cell of Co_2As.r [16] appeared, so that Co_2As.h transforming at 775 K to Co_2As.r [14] was presumably not quenched in our experiment.

The $Ni_{11}As_8$ phase does not dissolve much cobalt (Fig. 7); there appears no homogeneous connection to Co_3As_2.h. Perhaps CoAs.h(NiAs, [14]) is connected with NiAs (Fig. 8). The axial ratio of the H2.2 substructure changes continuously [10, 14] but all samples showed different superstructure lines indicated by S in Figs 5 and 8. While the composition is of strong influence on the additional lines, different quenching temperatures have no effect.

The phase Co_2As_3 (SR21.39) could not be found in powders quenched from 970 K. The section $Co_{1-N}Ni_NAs_2$ on quenching from 970 K gave broad

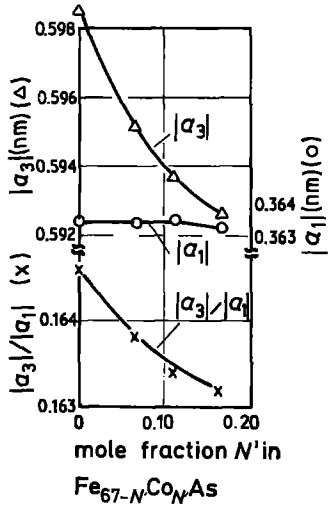

Figure 2 Cell of $Fe_{2-N}Co_NAs_1$ quenched from 870 K.

lines, so that our assumption in Fig. 5, which contradicts Naud and Breckpot [10] needs corroboration.

3. Open questions

Attempts to develop an energetical understanding of alloys such as those given here [8, 21–28] have given some insight into the phenomenological systematics of the structures, but could provide only few stability and structural arguments. For such a purpose a valence model is necessary, i.e. a model which allows asignation to a phase of a binding indicating a low value of internal energy. Such a model is the plural-correlations model [9, 17, 29]. It will be used to analyse the bindings of the phases of the marginal mixtures and to discuss with the help of these bindings some observations in the three-component mixtures. Reference to Schubert [9, 17] is recommended for the understanding of this analysis.

Some general problems arising from the empirical data of a mixture (1) and some special problems occurring in $FeAs_M$ (2), $CoAs_M$ (3), $NiAs_M$ (4), $FeCo_MAs_{M'}$ (5) and $CoNi_MAs_M$ (6) are:

1. Which correlations and harmonies give stability to the phases? Is the degree of occupation compatible with binding rules already known [9]? How do the electron distances d_b, d_e, d_c and the site number ratio $N'^{S(b)}_{S(e)}$ depend on the mole fraction N'_2? Are there physical properties which are compatible with the proposed binding?

2. Why is Fe_2As, compared to Fe.r, strongly strained? Why is FeAs no longer homeotypic to a close packing? Why is $FeAs_2$ outstandingly stable?

3. Why is Co_5As_2 only stable at elevated temperatures? What is the reason for the anomalous axial ratio of Co_2As.r? Why is CoAs of the short subtype of the MnP type?

4. Why, in $Ni_{11}As_8$, are all B correlations compressed along a_3? Why does NiAs have a higher decomposition temperature than $Ni_{11}As_8$? Why does $NiAs_2$ have a higher melting temperature than NiAs?

5. Why does Fe_2As substitute little cobalt for iron? Why does $|a_3|/|a_1|$ in $Fe_{2-N}Co_NAs$(T4.2) decrease with increasing N? Why is the Fe_2P type stabilized for higher N in $Fe_{2-N}Co_NAs$? Why does the long FeAs go continuously to the short CoAs? What is the cause of the nonlinearity in Fig. 4?

6. Why does CoAs.r substitute little nickel for cobalt? Is a phase $Co_{1-N}Ni_NAs_3$(B4.12) possible?

The binding proposals which help to answer the above questions are determined by the binding analysis

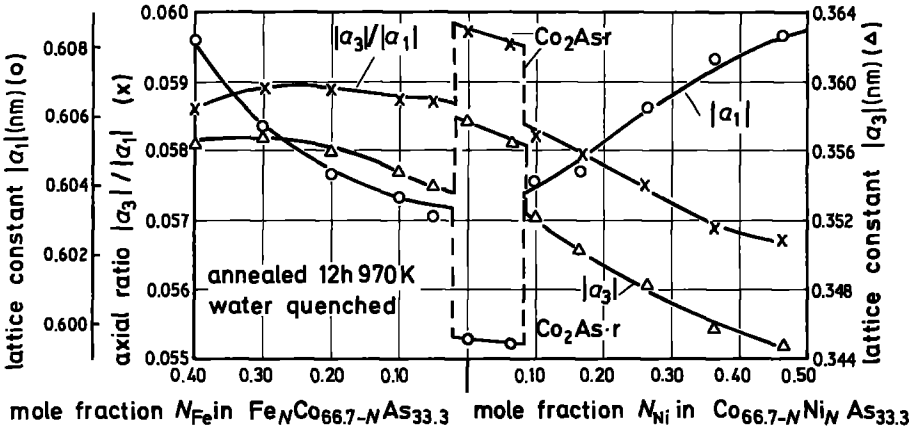

Figure 3 Cell of Co_2As.h with cobalt substituted by iron or nickel.

[9, 17] and they are noted in the following format:

(1) Name of the phase, (2) structure type, (3) structure reports reference (SR, volume, page), (4) electron numbers $N_b^{/a}$, $N_e^{/a}$, $N_c^{/a}$ in the cell a calculated with help of the electron count assumed for the mixture, (5) numerical value of the cell matrix a in abbreviated notation [9], (6) symbol b for the cell of the valence electron correlation, (7) index for the type of b, (8) brief notation of the commensurability $b^{-1}a$, (9) symbol e for the cell of the e correlation, (10) index for type of e, (11) commensurability $e^{-1}a$, (12–14) mostly omitted for brevity, symbol, type and commensurability of the c correlation (core electron correlation).

The distance values and site number ratios plotted in Figs 9, 11, 12 are deduced from the binding proposals by elementary calculation. These values are important for the assessment of the acceptability of the proposal. The smoothness of their dependence on the mole fraction suggests that the binding proposals are not ad hoc hypotheses, but real facilities of several spatial correlations to yield a low energy. Since many valence theories of alloys have been tried in the past without convincing success, it is advisable to examine any new attempt carefully. The conventional concept of a bond in a crystal is inconsistent in the opinion of the author,

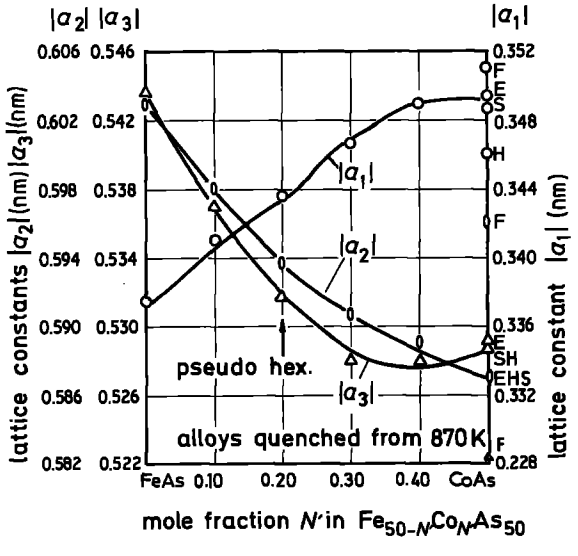

Figure 4 Cell of $Fe_{1-N}Co_NAs_1$(MnP) (E = own measurement, F = [48], H = [14], S = [52]).

as the problem of the interaction of the bonds has not been solved appropriately. The argument that the correlations have not yet been confirmed by direct experiment is not conclusive, as it requires a result which will probably emerge in the future, to be known already, while we cannot prescribe how the development of chemistry must run. In order to appreciate the following bindings. the change of the correlations and commensurabilities from phase to phase in the mixture should be carefully pursued.

4. Interpretation

Binding proposals for $FeAs_M$ may be derived from the electron count $Fe^{0,8,8}As_M^{5,0,10}$ and are the following (with comments annexed):

Fe.r(W, SR1.9198; 1.2, 14.8, 16)0.287 nm

$$= b_C(\sqrt{1.25};\ 1) = e_B^{\sim}\ (\sqrt{5};\ 1.92).$$

C is the cubic primitive and B the cubic body centred Bravais lattice. The e_B correlation is slightly strained ($\sim$) to give 19.2 e sites per cell and therefore 4.4 magnetons per cell in accordance with observation [30–32]. The reason for the strain is the necessity to depress the number of holes in the e correlation (d band). When the number surpasses the value 2.5 per atom, the e_B correlation would be destabilized, as one complete e layer is unoccupied. The $N_b^{/a}$ value 1.25 present in $FeAs_0$ will remain constant until the b contribution of iron is zero in agreement with Ekman's rule (see [8]). The binding must be twinned in a to generate the cubic symmetry; this is in accordance with the rule that for stability a harmony is sufficient in a plane. The occurrence of the root sign in the commensurabilities indicates that a rotation matrix tacitly had been omitted [9]. A similar binding was already found in [33]. With Fe.r is in equilibrium

$Fe_2As(Cu_2Sb,$ T4.2, SR21.43; 10, 32, 52)

$$0.363;\ 0.598\,\text{nm} = b_B^{\sim}\ (\sqrt{2};\ 2.5) = e_U(2;\ 4).$$

Fe_2As is a replacement and deformation homeotype of Fe.r ([8] drawing p. 320). The strong increase of the b^- electron number per atom has transformed b_C of Fe.r to $b_B^{\sim}$. As the e electron number per atom decreases, since arsenic does not contribute e electrons, an increase of d_e (Fig. 9) is caused. The good spin compensation of e_B (i.e. a + spin is a neighbour

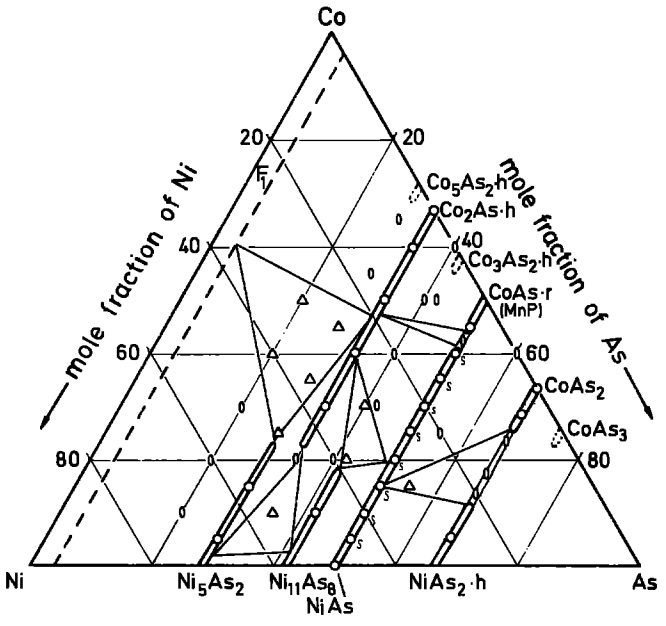

Figure 5 Phase diagram of $CoNi_MAs_{M'}$; 970 K. (○) One-phase, (0) two-phase, (△) three-phase alloy.

only to − spins) in Fe.r is also lost. The fully occupied and well commensurable e_U correlation does not allow much cobalt to be substituted for iron. Since the compliant directions of e_U lie in the a_1, a_2 plane it is clear that the axial ratio $|a_3|/|a_1|$ must decrease with increasing cobalt content following the rule of straining [9]. The structure replacing the Cu_2Sb type of Fe_2As in $Fe_{2-N}Co_NAs$ at higher cobalt contents is the Fe_2P type of $Co_2As.h$. While $Co_2As.h$ has $N_{S(e)}^{/At} = 6.3\,e$ sites per atom (see below), Fe_2As has $N_{S(e)}^{/At} = 5.3$, and therefore becomes less appropriate than the Fe_2P type at higher cobalt content. The next phase is [48]

$$\text{FeAs(MnP, O4.4, SR21.43; 20, 32, 72)}$$

$$0.337;\ 0.602;\ 0.543\,\text{nm} = b_{FHQ}(2/2;\ 3;\ 3.4/3)$$

$$= e_{FHQ}(2;\ 4/2;\ 4/3).$$

FeAs(MnP, [8] drawing p. 331) is DI-homeotypic to NiAs (D = homogeneous deformation, I = inhomogeneous deformation) with the commensurability $a = a_{NiAs}\,(1, -1, 0;\ 1, 1, 0;\ 0, 0, 1)$. F_{HQ} (written in the fomula FHQ) is the face centred cubic type first taken in hexagonal aspect (H) and then in orthorhombic one face centred aspect (Q). Some commensurability elements are written as fractions to identify the number of electron layers per a_i vector. A better spin compensation could be reached by interpreting e_{FHQ} as slightly strained $e_{UHQ}^{\sim}$, i.e. by changing the e stacking. U is tetragonal body centred with axial ratio 0.82 [9]. The low site number ratio $N_{S(e)}^{/S(b)} = 1.6$ no longer allows a close packed crystal structure. The commensurability $b^{-1}a$ may be named a $(\sqrt{3})$-commensurability to the basal hexagonal a submesh and $e^{-1}a$ a $(\sqrt{4})$-commensurability (Fig. 10), and the coexistence of both is the building principle of the $MgCu_2$ homeotypes [34]. The binding in FeAs is therefore remotely homeotypic to $MgCu_2$. The sites of difficult fit of b and e (Fig. 10) probably introduce momentary electrical dipoles in the a_2 direction and these cause a kinking in the a_2 direction of A atom chains along a_3. This kinking appears more probable when the e_{FH} correlation is interpreted as an $e_{UH}^{\sim}$ correlation strained somewhat in the a_3 direction. Since the A chains are not symmetrically but antisymmetrically kinked (see [8] drawing p. 331) to reduce the energy of the electrical dipoles, the a cell is strained in the a_2 direction so that the structure belongs to the "long" subtype of the MnP type [8].

The continuous transition of the long FeAs to the short CoAs may be rationalized as follows. When the e concentration $N_e^{/At}$ is increased in FeAs by substitution of cobalt for iron, then new e planes must be inserted perpendicular to the most compliant direction of b which is probably a_1 (see [8] p. 99).

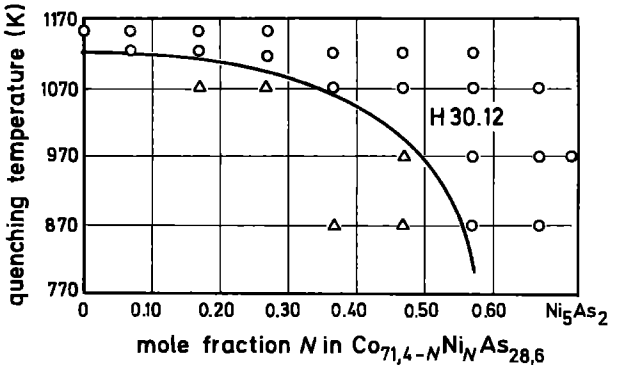

Figure 6 Homogeneity range of $Co_{5-N}Ni_NAs_2$.

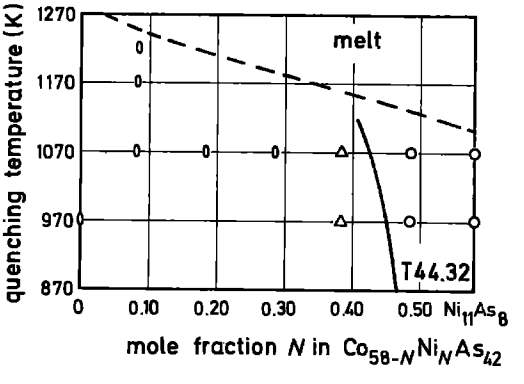

Figure 7 The $Co_{11-N}Ni_NAs_8$ phase.

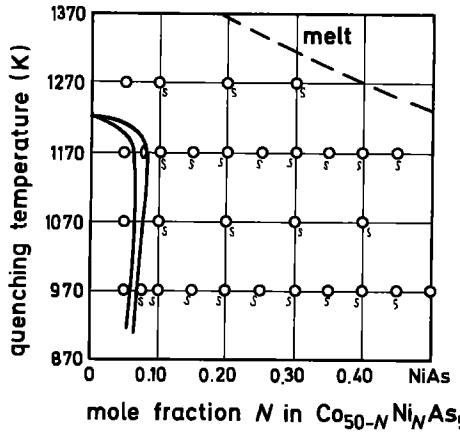

Figure 8 Homogeneity range of $Co_{1-N}Ni_NAs_1$, S = contains superstructure.

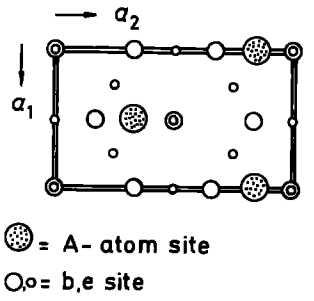

Figure 10 Coexistence of a hexagonal atom lattice with a hexagonal electron configuration causes an orthorhombic crystal. The critical region where the basal coordinates of *b* and *e* sites coincide impresses an orthorhombic symmetry on the *a* lattice. Since it approximately repeats in every *e* layer parallel to a_1, a_2 it tends to kink the A chains parallel to a_3 in the a_2 direction.

Therefore a_1 is strained with increasing N'_{Co}, so that the cell eventually becomes pseudohexagonal, and then of the short subtype. This is, in fact, observed in $Fe_{1-N}Co_NAs$. In addition the binding is compatible with the rule of Rundqvist [20] that at a given *e* concentration pseudo-hexagonality is attained. Therefore Rundqvist's rule sustains, together with many binding analyses [28], the above noted electron count. For the next phase a remarkable binding proposal may be found

$FeAs_2$(FeS$_2$.r, SR33.63; 20, 16, 56) 0.288; 0.598;

0.530 nm = $b^{\sim}_{UHQ}(2/2; 3; 3/2) = e^{\sim}_{UHQ}(2/2; 3; 3/2)$

The structure ([8] drawing p. 434) is L-homeotypic to FeAs (L = lacuna = constitutional vacancy), but the strongly contracted a_1 axis indicates a somewhat different binding. Remarkably a "short" $NiAs_2$.h with $|a_2|/\sqrt{3}|a_1| = 0.95$ belongs to the "long" $FeAs_2$ with $|a_2|/\sqrt{3}|a_1| = 1.20$ [35–39]. The mechanism to generate this homeotypism to MnP is similar to that in the MnP type.

Binding proposals for $CoAs_M$ may be derived from the electron count $Co^{0,9,8}As_M^{5,0,10}$, and are:

Co.h(Cu, SR18.118; 2.4, 33.6, 32)0.354 nm

= $b_C(\sqrt{2}; 1.4) = e^{\sim}_B(\sqrt{8}; 2.5)$.

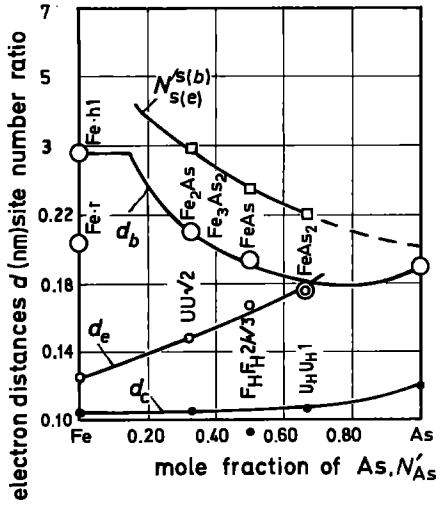

Figure 9 Electron distances and site number ratio of $FeAs_M$ in dependence of the mole fraction N'_{As}, (binding diagram).

It is seen that 1.7 holes in the d band correspond to the observation [30]. The deformation of e_B corresponds to the full occupation of the + spin d band, i.e. to Hund's rule. For the room temperature phase we find:

Co.r(Mg, SR22.101; 1.4, 16.6, 16) H0.251;

0.407 nm = $b_H(1; 1.66) = e^{\sim}_{UH}(2; 5/2)$.

The number of holes per atom in the d band is 1.8, the $e^{\sim}_{UH}$ correlation is somewhat overcompressed. When the *e* layers are smeared out parallel to the basal planes of *a*, then alternating electro dipoles in the a_3 direction are formed at the atoms which favour the magnesium type stacking of atomic layers (following Schubert [34]). The next phase yields the binding:

Co_5As_2.h(Pd_5Sb_2, H30.12, [11]; 60, 270, 330)

H0.6797; 1.2423 nm = $b_{FH}(3; 6.7/3)$

= $e^{\sim}_{UH}(\sqrt{27}; 12/2)$.

The phase (drawing [12]) is homeotypic to Ni_2In with the commensurability $a = a_{Ni2In}(\sqrt{3}; 2.5)$. The main advantage of the binding is the excellent commensurability of b_{FH} to the atomic sites. The *c* correlation $a = c_{CH}(\sqrt{27}; 24/3)$ also fits *e* well. The phase is unstable at lower temperatures probably as cobalt absorbs *b* electrons and destroys the good commensurability.

The next phase Co_2As exhibits a change of axial ratio. It appears that in the above experiments on $Co_{67}As_{33}$, Co_2As.r [14, 16] was always obtained which yields the binding:

Co_2As.r(Fe_2P, H6.3, SR21.38; 15, 54, 78)

H0.597; 0.358 nm = $b_{FH}(\sqrt{7}; 2/3)$

= $e_{BH}(\sqrt{7}; 7.8/3)$.

Probably this phase necessitates absorption of *b* electrons by cobalt. However, when the mole fraction $N'_{Ni} > 0.1$ the Co_2As.h type appears (Fig. 3, Table II) and for this

Co_2As.h(Fe_2P, H6.3, SR21.39; 15, 54, 78)

H0.606; 0.356 nm = $b_{CH}(\sqrt{4.75}; 3/3)$

= $e_{FH}(\sqrt{19}; 3/3)$

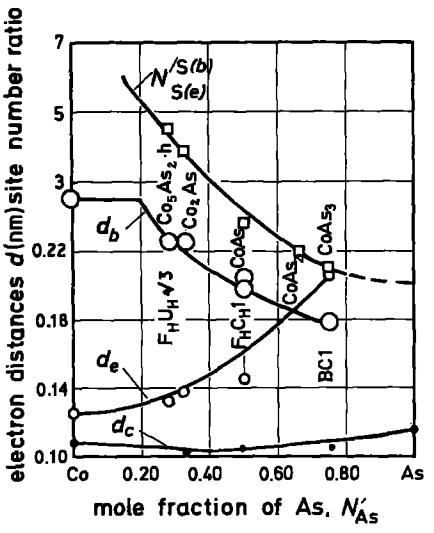

Figure 11 Binding diagram of $CoAs_M$.

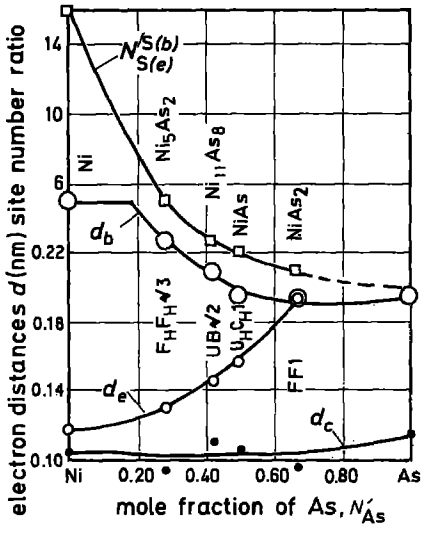

Figure 12 Binding diagram of $NiAs_M$.

may be assumed. Here e_{FH} may be interpreted as $e^{\sim}_{UH}$ to have better spin compensation. It is seen that the commensurability ($\sqrt{19}$; 3/3) offers more sites than ($\sqrt{7}$; 7.8/3). In equilibrium with Co_2As is

CoAs.h(NiAs, H2.2, SR21.39; 10, 18, 36)

H0.356; 0.522 nm = $b^{\sim}_{FH}(\sqrt{3}; 3.3/3)$

= $e_{CH}(\sqrt{3}; 6/3)$.

At lower temperatures e_{CH} of CoAs.h will tend to $e^{\sim}_{FH}$ which is closer packed. The phase CoAs.r [52] must be homeodesmic to FeAs:

CoAs.r(MnP, SR21.39; 20, 36, 72)

0.353; 0.589; 0.517 nm = $b_{FHQ}(2.1/2; 3; 3.2/3)$

= $e^{\sim}_{UHQ}(2.2; 4/2; 4/2)$.

The deformation of the a_1, a_2 plane as compared with CoAs.h speaks in favour of $e^{\sim}_{UH}$ as this correlation contains a tendency to deformation when it is not twinned. It is satisfactory that CoAs.r does not substitute much nickel for cobalt as the possibility of straining the cell a is exhausted in CoAs.r. In CoAs.r the axial ratio $|a_2|/|a_1|$ decreases with external pressure and in FeAs it increases [40]. This may be connected with the nonlinear effect in Fig. 4 which stops the increase of a_1 with increasing e electron concentration.

The $CoAs_2$ phase ($CoSb_2$ [41]) is homeotypic to FeS_2.r, and Fig. 11 suggests that its stability comes from $N_b^{/CoAs_2} \approx N_e^{/CoAs_2}$ resulting in congruence of b and e. For $CoAs_3$ ([5], [8] drawing p. 348) we obtain

$CoAs_3$(B4.12, SR37.14; 120, 72, 304)0.8195 nm

= $b_B(4) = e_C(4) = c_C(8)$.

Evidently eight d electrons are excited into the b correlation. Following this binding a "$NiAs_3$(B4.12)" is not possible because of the electron numbers.

Binding proposals for $NiAs_M$ may be derived from the electron count $Ni^{0,10,8}As_M^{5,0,10}$ as follows:

Ni(Cu, SR1.68; 2.4, 37.6, 32)0.352 nm

= $b_2(\sqrt{2}; 1.2) = e^{\sim}_B(\sqrt{8}; 2.5)$.

The tetragonally deformed e correlation is confirmed by the compressed axial ratio of the tetragonal Pd_3In [42], Pd_3Tl [43], and $Pd_{3.1}Sn$ [44]. The binding must be twinned in a. The phase $Ni_5As_2(Pd_5Sb_2)$ [12] is isodesmic to $Co_5As_2(Pd_5Sb_2)$, it may be added that the rule of the uniform distribution of the b electron-rich atoms [45] is obeyed.

The $Ni_{11}As_8$ phase [46] suggests the binding proposal:

$Ni_{11}As_8$(T44.32, SR39.12; 160, 440, 672) 0.687;

2.182 nm = $b^{\sim}_B(\sqrt{8}; 10) = e^{\sim}_B(4; 14)$

= $c_B(\sqrt{32}; 20)$.

The three correlations fit excellently together. All B types are compressed in order to attain a higher density. They cannot be compressed to the U type as this type does not give a good spin compensation.

In equilibrium with $Ni_{11}As_8$ is

NiAs(H2.2, SR1.84; 10, 20, 36) H0.362;

0.503 nm = $b^{\sim}_{UH}(\sqrt{3}; 3.3/2) = e^{\sim}_{CH}(\sqrt{3}; 6.6/3)$

= $c_H(\sqrt{12}; 5)$.

The proposal is an improvement of a proposal which did not obey Ekman's rule [28]. The site number ratio has decreased to 2. The fuction $N^{/S(b)}_{S(e)}(N'_{As})$ tends to zero for $N'_{As} = 1$. The high compliance of e becomes evident from Fig. 12. It may be extrapolated from Fig. 12 that $NiAs_2$ has a XX1 binding (X = F or B or . . .)

$NiAs_2$.h(FeS_2.r, SR33.63; 20, 20, 56) 0.355; 0.579;

0.476 nm = $b_{FHQ}(2.2/2; 3; 3/3) = e_{FHQ}(2.2/2; 3; 3/3)$

The 1-factoriality (congruence) of the correlations causes a high melting temperature [13, 47] following the rule of commensurability [9, 17].

For $NiAs_2$.r($AuSn_2$, [8] drawing p. 347) [49–51] comes a homeotypic binding

$NiAs_2$.r(O8.16, SR33.34, 38.27; 80, 80, 224)

0.575; 0.580;1.141 nm = $b^{\sim}_{FU}(3; 9/2)$

= $e^{\sim}_{FU}(3; 9/2)$,

The weak deformation of *b* and *e* probably serves to improve the spin compensation.

References

1. K. FRIEDRICH, *Metallugie* **4** (1907) 129.
2. *Idem, ibid.* **5** (1908) 150.
3. *Idem, ibid.* **4** (1907) 202.
4. G. AMINOFF, *Z. Krist.* **58** (1923) 203.
5. I. OFTEDAL, *ibid.* **66** (1928) 517.
6. G. HÄGG, *ibid.* **71** (1929) 134.
7. M. ELANDER, G. HÄGG and A. WESTGREN, *Ark. Kemi-Mineral. Geol.* **12B** (1935) No. 1.
8. K. SCHUBERT, "Kristallstr. zweikomponentiger Phasen", Berlin (1964).
9. K. SCHUBERT, *Z. Krist.* **165** (1983) 23.
10. J. NAUD and R. BRECKPOT, *Bull. Soc. Chim. Belges* **81** (1972) 247.
11. M. ELLNER, E. LUKAČEVIĆ and M. El-BORAGY, *J. Less-Common Metals* **118** (1986) 327.
12. M. El-BORAGY, S. BHAN and K. SCHUBERT, *ibid.* **22** (1970) 445.
13. R. A. YUND, *Econ. Geol.* **56** (1961) 1273.
14. R. D. HEYDING and L. D. CALVERT, *Can. J. Chem.* **35** (1957) 449.
15. S. RUNDQVIST and F. JELLINEK, *Acta Chem. Scand.* **13** (1959) 425.
16. A. NYLUND, A. ROGER, J. P. SENATEUR and R. FRUCHART, *J. Solid State Chem.* **4** (1972) 115.
17. K. SCHUBERT, *Commun. Math. Chem.* **19** (1968) 287.
18. IUPAC, "Nomenclature of Inorganic Chemistry" (Butterworths, London, 1971).
19. HANSEN-ANDERKO, "Constitution of Binary Alloys" (New York, 1958) p.163.
20. St. RUNDQVIST, *Acta Chem. Scand.* **16** (1962) 287.
21. G. S. ZHDANOV and V. P. GLAGOLEVA, *Trudy Inst. Kristallogr.* **ANSSSR9** (1954) 211.
22. F. HULLIGER, *Struct. Bonding* **4** (1968) 83.
23. W. B. PEARSON, "The Crystal Chemistry and Physics of Metals and Alloys" (Wiley, New York, 1972).
24. F. JELLINEK, *MTP Int. Rev. Sci. Inorg. Chem. Ser. 1,* **5** (1972) 339.
25. A. F. WELLS, "Structural Inorganic Chemistry" (Clarendon, Oxford, 1975).
26. H. F. FRANZEN, *Progr. Solid State Chem.* **12** (1978) 1.
27. F. HULLIGER, in "Structure and Bonding in Crystals" (edited by M. O'Keefe and A. Navrotsky, Academic, New York, 1981).
28. K. SCHUBERT, *Commun. Math. Chem.* **17** (1985) 219.
29. *Idem, J. Less-Common Metals* **70** (1980) 167.
30. N. F. MOTT and H. JONES, "Theory of Properties of Metals and Alloys" (Oxford University Press, 1936).
31. P. W. SELWOOD, "Magnetochemistry" (Interscience, New York, 1943).
32. E. KNELLER, "Ferromagnetismus" see Appendix by A. Seeger and H. Kronmüller (Springer Verlag, Berlin, 1962).
33. K. SCHUBERT, *Arch. Eisenhüttenw.* **26** (1955) 299.
34. K. SCHUBERT, *J. Solid State Chem.* **53** (1984) 246.
35. M. J. BUERGER, *Amer. Mineral.* **22** (1937) 48.
36. *Idem, Z. Krist.* **97** (1937) 504.
37. W. JEITSCHKO, *Acta Cryst.* **B30** (1974) 2565.
38. A. KJEKSHUS and T. RAKKE, *Structure and Bonding* **19** (1974) 85.
39. M. E. FLEET, *Z. Krist.* **142** (1975) 332.
40. P. S. LYMAN and C. T. PREWITT, *Acta Cryst.* **B40** (1984) 14.
41. A. KJEKSHUS, *Acta Chem. Scand.* **25** (1971) 411.
42. S. BHAN and K. SCHUBERT, *J. Less-Common Metals* **17** (1969) 73.
43. S. BHAN, T. GÖDECKE, P. K. PANDAY and K. SCHUBERT, *ibid.* **16** (1968) 415.
44. K. SCHUBERT, H. L. LUKAS, H. G. MEIßNER and S. BHAN, *Z. Metallkde.* **50** (1959) 534.
45. W. WOPERSNOW and K. SCHUBERT, *J. Less-Common Metals* **41** (1975) 94.
46. M. E. FLEET, *Amer. Mineral* **58** (1973) 203.
47. F. A. SHUNK, "Constitution of Binary Alloys", 2nd Supplement (McGraw-Hill, New York, 1969).
48. K. E. FYLKING, *Ark. Kemi Min. Geol.* **11B** (1934) Nr. 48.
49. W. N. STASSEN and R. D. HEYDING, *Canad. J. Chem.* **46** (1968) 2159.
50. H. HOLSETH and A. KJEKSHUS, *Acta Chem. Scand.* **22** (1968) 3284.
51. M. E. FLEET, *Amer. Mineral* **57** (1972) 1.
52. K. SELTE and A. KJEKSHUS, *Acta Chem. Scand.* **25** (1971) 3277.

Received 9 December 1985
and accepted 14 March 1986